ЖЭТФ, 2005, том 127, вып. 4, стр. 1–12

SYNCHRONIZATION OF CHAOTIC OSCILLATOR TIME SCALES

A. E. Hramov**, A. A. Koronovskii, Yu. I. Levin

Saratov State University
410012, Saratov, Russia

Submitted 18 June 2004

We consider the chaotic oscillator synchronization and propose new approach for detecting the synchronized behavior of chaotic oscillators. This approach is based on the analysis of different time scales in the time series generated by coupled chaotic oscillators. We show that complete synchronization, phase synchronization, lag synchronization, and generalized synchronization are particular cases of the synchronized behavior called the time-scale synchronization. The quantitative measure of the chaotic oscillator synchronous behavior is proposed. This approach is applied for the coupled Rössler systems.

PACS: 05.45.Xt, 05.45.Tp

1. INTRODUCTION

Synchronization of chaotic oscillators is one of the fundamental phenomena in nonlinear dynamics. It occurs in many physical [1–6] and biological [7–9] processes. It seems to play an important role in the ability of biological oscillators, such as neurons, to act cooperatively [10–12].

Several different types of synchronization of coupled chaotic oscillators have been described theoretically and observed experimentally [13–16]. The complete synchronization implies the coincidence of states of coupled oscillators, $\mathbf{x}_1(t) \approx \mathbf{x}_2(t)$, with the difference between state vectors of coupled systems converging to zero in the limit as $t \to \infty$ [17–20]. It occurs when interacting systems are identical. If the parameters of coupled chaotic oscillators slightly mismathch, the state vectors are close, $|\mathbf{x}_1(t) - \mathbf{x}_2(t)| \approx 0$, but differ from each other. Another type of synchronized behavior of coupled chaotic oscillators with slightly mismatched parameters is the lag synchronization: this is the case where the state vectors coincide with each other after a time shift, $\mathbf{x}_1(t+\tau) = \mathbf{x}_2(t)$. As the coupling between the oscillators increases, the time lag τ decreases and the synchronization regime tends to the one [21–23]. The generalized synchronization [24–26], introduced for drive-response systems, means that there is some functional relation between coupled chaotic oscillators, i.e., $\mathbf{x}_2(t) = \mathbf{F}[\mathbf{x}_1(t)]$.

We finally mention the phase synchronization regime. To describe the phase synchronization, the instantaneous phase $\phi(t)$ of a chaotic continuous time series is usually introduced [13–16, 27, 28]. The phase synchronization means the entrainment of phases of chaotic signals, with their amplitudes remaining chaotic and uncorrelated.

All synchronization types mentioned above are related with each other (see [1, 22, 24] for details), but the relation between them is not completely clarified yet. For each type of synchronization, there are specific ways to detect the synchronized behavior of coupled chaotic oscillators. The complete synchronization can be detected comparison of system state vectors $\mathbf{x}_1(t)$ and $\mathbf{x}_2(t)$, whereas the lag synchronization can be determined by means of a similarity function [21]. The case of the generalized synchronization is more intricate because the functional relation $\mathbf{F}[\dots]$ can be very complicated, but there are several methods to detect the synchronized behavior of coupled chaotic oscillators, such as the auxiliary system approach [29] or the method of nearest neighbors [24, 30].

Finally, the phase synchronization of two coupled chaotic oscillators occurs if the difference between the instantaneous phases $\phi(t)$ of chaotic signals $\mathbf{x}_{1,2}(t)$ is bounded by some constant:

$$|\phi_1(t) - \phi_2(t)| < \text{const}. \qquad (1)$$

It is possible to define the mean frequency of the chaotic signal,

*E-mail: aeh@cas.ssu.runnet.ru

$$\bar{\Omega} = \lim_{t\to\infty} \frac{\phi(t)}{t} = \langle \dot{\phi}(t) \rangle, \qquad (2)$$

which is the same for both coupled chaotic systems, i.e., phase locking leads to frequency entrainment. We note that for the results to be correct, the mean frequency $\bar{\Omega}$ a of chaotic signal $\mathbf{x}(t)$ must coincide with the main frequency $\Omega_0 = 2\pi f_0$ of the Fourier spectrum (see [31] for details]). There is no general way to introduce the phase for chaotic time series. There are several approaches that allow defining the phase for «good» systems with a simple topology of a chaotic attractor (the so-called phase coherent attractor), whose Fourier spectrum contains a single main frequency f_0.

First of all, a plane in the system phase space may exist such that the projection of the chaotic attractor on it looks like a circular band. For such a plane, the coordinates x and y can be introduced with the origin placed somewhere near the center of the chaotic attractor projection. The phase can then be introduced as an angle in this coordinate system [32, 21], but this requires all trajectories of the chaotic attractor projection on the (x, y) plane to revolve around the origin. A coordinate transformation can be sometimes used to obtain a proper projection [32, 13]. If the projections of chaotic trajectories on the plane $(\dot{x}, \dot{y})$ always rotate around the origin, the velocities $\dot{x}$ and $\dot{y}$ can also be used; in some cases, this approach is more suitable [33, 34]. Another way to define the phase $\phi(t)$ of a chaotic time series $x(t)$ is to construct the analytical signal [14, 27] using the Hilbert transform. Moreover, the Poincaré secant surface can be used to introduce the instantaneous phase of a chaotic dynamical system [14, 27]. Finally, the phase of a chaotic time series can be introduced by means of the continuous wavelet transform [35], but the appropriate wavelet function and its parameters should be chosen [36].

All these approaches give correct results for «good» systems with well-defined phase, but fail for oscillators with nonrevolving trajectories. Such chaotic oscillators are often called «systems with ill-defined phase». Introducing the phase via the approaches mentioned above usually leads to incorrect results for system with ill-defined phase [31]. Therefore, the PS of such systems can be usually detected by means of indirect indications [32, 37] and measurements [33].

In this paper, we propose a new approach for detecting the synchronization between two coupled chaotic oscillators. The main idea of this approach consists in the analysis of the system behavior at different time scales, which allows us to consider different cases of synchronization from a universal standpoint [38]. Using the continuous wavelet transform [39–42], we introduce the continuous set of time scales s and the instantaneous phases $\phi_s(t)$ associated with them. In other words, $\phi_s(t)$ is a continuous function of time t and time scale s. As we show in what follows, if two chaotic oscillators demonstrate any type of synchronized behavior mentioned above, the time series $\mathbf{x}_{1,2}(t)$ generated by these systems involve time scales s that are necessarily correlated and satisfy the phase locking condition

$$|\phi_{s1}(t) - \phi_{s2}(t)| < \text{const}. \qquad (3)$$

In other words, complete, lag, phase, and generalized synchronizations are the particular cases of the synchronous coupled chaotic oscillator behavior called «time-scale synchronization».

The structure of this paper is as following. In Sec. 2, we discuss the continuous wavelet transform and the method of the time scales s and define the phases $\phi_s(t)$ associated with them. In Sec. 3, we consider the phase synchronization of two coupled Rössler systems. We demonstrate the application of our method and discuss its relation to traditional approaches. Section 4 deals with synchronization of two coupled Rössler systems with funnel attractors. In this case, the traditional methods for introducing the phase fail and it is impossible to detect the phase synchronization regime. Synchronization between systems can be revealed here only by means of indirect measurements (see [33] for details). We demonstrate the efficiency of our method for such cases and discuss the correlation between phase, lag, and complete synchronizations. In Sec. 5, we apply our method to the unidirectional coupled Rössler systems in which the generalized synchronization is observed. The quantitative measure of synchronization is described in Sec. 6. The conclusions are presented in Sec. 7.

2. CONTINUOUS WAVELET TRANSFORM

The continuous wavelet transform is a powerful tool for analyzing the behavior of nonlinear dynamical systems. In particular, the continuous wavelet analysis has been used for the detection of synchronization of chaotic oscillations in the brain [35, 43, 44] and chaotic laser array [45]. It has also been used to detect the basic frequency of oscillations in nephron autoregulation [46]. We propose to analyze the dynamics of coupled chaotic oscillators by considering system behavior at different time scales s, each of which is characterized by its own phase $\phi_s(t)$. In defining the continuous set of instantaneous phases $\phi_s(t)$, the continuous wavelet transform is therefore a convenient mathematical tool.

We consider the continuous wavelet transform of a chaotic time series $x(t)$,

$$W(s,t_0) = \int\limits_{-\infty}^{\infty} x(t)\psi^*_{s,t_0}(t)\,dt, \tag{4}$$

where $\psi_{s,t_0}(t)$ is the wavelet function related to the mother-wavelet function $\psi_0(t)$ as

$$\psi_{s,t_0}(t) = \frac{1}{\sqrt{s}}\psi\left(\frac{t-t_0}{s}\right). \tag{5}$$

The time scale s corresponds to the width of the wavelet function $\psi_{s,t_0}(t)$, t_0 is the shift of the wavelet along the time axis, and the symbol «$*$» in (4) denotes complex conjugation. We note that the time scale s is typically used instead of the Fourier-transform frequency f and can be considered as the quantity inversed to it.

The Morlet wavelet [47]

$$\psi_0(\eta) = \frac{1}{\sqrt[4]{\pi}}\exp(j\Omega_0\eta)\exp\left(-\frac{\eta^2}{2}\right) \tag{6}$$

has been used as a mother-wavelet function. The choice of the parameter value $\Omega_0 = 2\pi$ provides the relation $s = 1/f$ between the time scale s of the wavelet transform and the frequency f of the Fourier transform.

The wavelet surface

$$W(s,t_0) = |W(s,t_0)|\exp[j\phi_s(t_0)] \tag{7}$$

describes the system dynamics on every time scale s at the time instant t_0. The value of $|W(s,t_0)|$ indicates the presence and intensity of the time scale s mode in the time series $x(t)$ at the time instant t_0. The quantities

$$E(s,t_0) = |W(s,t_0)|^2 \tag{8}$$

and

$$\langle E(s)\rangle = \int |W(s,t_0)|^2\,dt_0 \tag{9}$$

are the instantaneous and integral energy distributions on time scales, respectively.

The phase $\phi_s(t) = \arg W(s,t)$ is naturally introduced for every time scale s. This means that the behavior of each time scale s can be described by means of its own phase $\phi_s(t)$. If two interacting chaotic oscillators are synchronized, the corresponding time series $\mathbf{x}_1(t)$ and $\mathbf{x}_2(t)$ involve scales s correlated with each other. This correlation can be detected by examining condition (3), which must be satisfied for synchronized time scales.

3. PHASE SYNCHRONIZATION OF TWO RÖSSLER SYSTEMS

We first consider two coupled Rössler systems with slightly mismatched parameters [27, 28],

$$\begin{aligned}
\dot{x}_{1,2} &= -\omega_{1,2}y_{1,2} - z_{1,2} + \varepsilon(x_{2,1} - x_{1,2}),\\
\dot{y}_{1,2} &= \omega_{1,2}x_{1,2} + ay_{1,2},\\
\dot{z}_{1,2} &= p + z_{1,2}(x_{1,2} - c),
\end{aligned} \tag{10}$$

where $a = 0.165$, $p = 0.2$, and $c = 10$. The parameters $\omega_{1,2} = \omega_0 \pm \Delta$ determine the parameter detuning and ε is the coupling parameter ($\omega_0 = 0.97$, $\Delta = 0.02$). It was shown [21] that the PS is observed for these control parameter values and the coupling parameter $\varepsilon = 0.05$.

In this case, the phase of the chaotic signal can be easily introduced in one of the ways mentioned above, because the phase coherent attractor with rather simple topological properties is realized in the system phase space. The attractor projection on the (x,y) plane resembles the smeared limit cycle where the phase point always rotates around the origin (Fig. 1*a*). The Fourier spectrum $S(f)$ contains the basic frequency peak $f_0 \approx 0.163$ (see Fig. 1*b*), which coincides with the mean frequency $\bar{f} = \bar{\Omega}/2\pi$ determined from the instantaneous phase $\phi(t)$ dynamics (2). Therefore, the phase synchronization regime can be detected in two coupled Rössler systems (10) by means of traditional approaches without complications.

When the coupling parameter ε is equal to 0.05, the PS between chaotic oscillators is observed. Phase locking condition (1) is satisfied and the mean frequencies $\bar{\Omega}_{1,2}$ are entrained. Hence, the time scales $s_0 \approx 6$ of both chaotic systems corresponding to the mean frequencies $\bar{\Omega}_{1,2}$ should be correlated with each other. Correspondingly, the phases $\phi_{s1,2}(t)$ associated with these time scales s should be locked and condition (3) should be satisfied. The time scales that are nearest to the time scale s_0 should also be correlated, but the interval of the correlated time scales depends on the coupling strength. At the same time, there should be time scales that remain uncorrelated. These uncorrelated time scales cause a difference between chaotic oscillations of coupled systems.

Figure 2 illustrates the behavior of different time scales for two coupled Rössler systems (10) with phase coherent attractors. It is clear that the phase difference $\phi_{s1}(t) - \phi_{s2}(t)$ for scales $s_0 = 6$ is bounded, and therefore time scales $s_0 = 6$ corresponding to the main frequency f_0 of the Fourier spectrum are synchronized. It is important to note that the wavelet power spectra $\langle E_{1,2}(s)\rangle$ that are close to each other (Fig. 2*a*) and time scales s characterized by a large value of energy

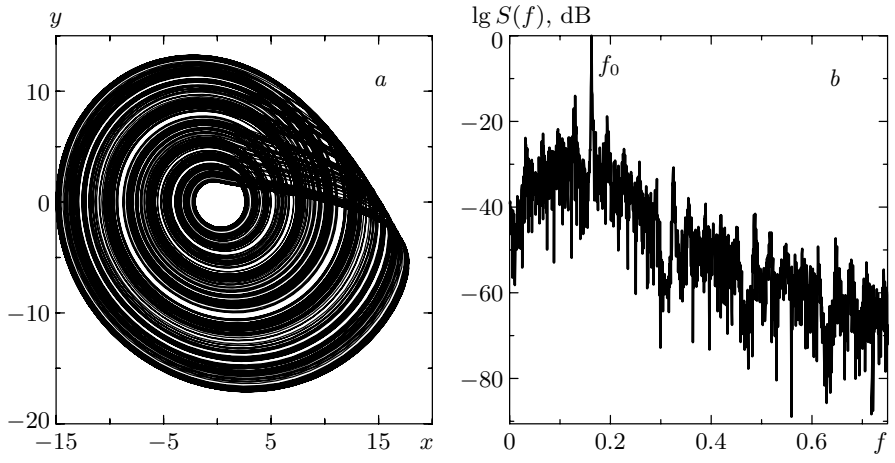

Fig. 1. (a) A phase coherent attractor and (b) the Fourier spectrum for the first Rössler system (10). The coupling parameter ε between the oscillators is equal to zero

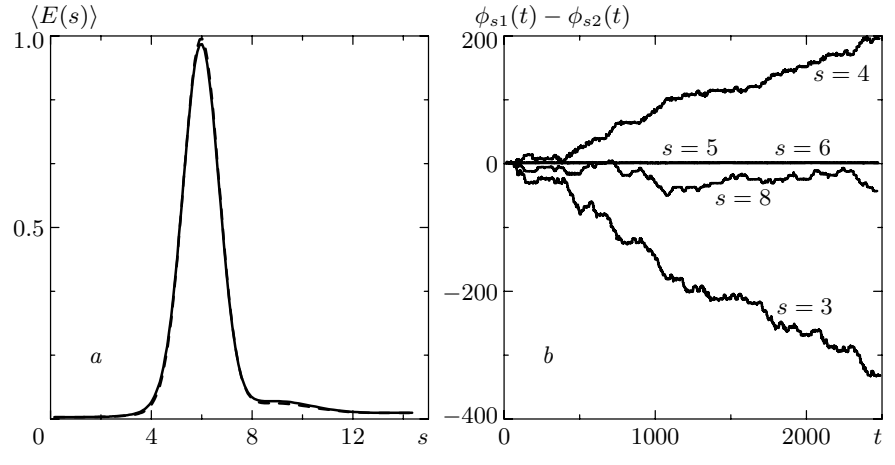

Fig. 2. (a) Wavelet power spectra $\langle E(s)\rangle$ for the first (solid line) and the second (dashed line) Rössler systems (10). (b) The dependence of the phase difference $\phi_{s1}(t) - \phi_{s2}(t)$ on time t for different time scales s. The coupling parameter between the oscillators is $\varepsilon = 0.05$. Phase synchronization for two coupled chaotic oscillators is observed

(e.g., $s = 5$) close to the main time scale $s_0 = 6.0$ are also correlated. There are also time scales that are not synchronized, for example, $s = 3.0$, $s = 4.0$ (Fig. 2b).

Therefore, phase synchronization of two coupled chaotic oscillators with phase coherent attractors manifests itself as a synchronous behavior of the time scales s_0 (and time scales s close to s_0) corresponding to the chaotic signal mean frequency $\bar{\Omega}$.

4. SYNCHRONIZATION OF TWO RÖSSLER SYSTEMS WITH FUNNEL ATTRACTORS

We consider a more complicated example where it is impossible to correctly introduce the instantaneous phase $\phi(t)$ of the chaotic signal $\mathbf{x}(t)$. It is clear that in such cases, the traditional methods of detecting the phase synchronization fail and it is necessary to use the other techniques, e.g., indirect measurements [33]. On the contrary, our approach gives correct results and allows detecting the synchronization between chaotic oscillators as easily as before.

As an illustration, we consider two nonidentical coupled Rössler systems with funnel attractors (Fig. 3),

$$\begin{aligned} \dot{x}_{1,2} &= -\omega_{1,2} y_{1,2} - z_{1,2} + \varepsilon(x_{2,1} - x_{1,2}), \\ \dot{y}_{1,2} &= \omega_{1,2} x_{1,2} + a y_{1,2} + \varepsilon(y_{2,1} - y_{1,2}), \\ \dot{z}_{1,2} &= p + z_{1,2}(x_{1,2} - c), \end{aligned} \tag{11}$$

where ε is a coupling parameter and $\omega_1 = 0.98$,

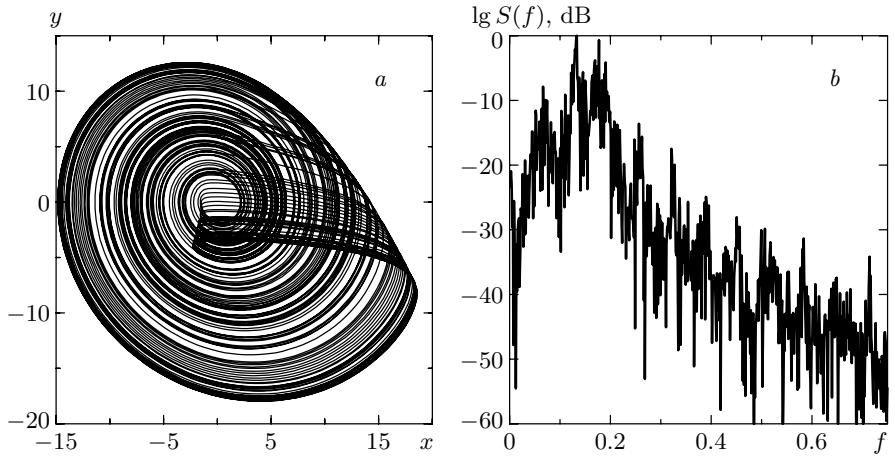

Fig. 3. (a) A phase picture and (b) the power spectrum of oscillation for the first Rössler system (11). The coupling parameter ε is equal to zero

$\omega_2 = 1.03$. The control parameter values have been selected by analogy with [33] as $a = 0.22$, $p = 0.1$, and $c = 8.5$. We note that under these control parameter values, none of the methods mentioned above allows defining the phase of the chaotic signal correctly in entire range of the coupling parameter ε variation. Therefore, nobody can determine by means of direct measurements whether the synchronization regime occurs for several values of ε. On the other hand, our approach allows easily detecting synchronization between the coupled oscillators under consideration for all values of the coupling parameter.

In [33], was shown by means of indirect measurements that for the coupling parameter value $\varepsilon = 0.05$, synchronization of two coupled Rössler systems (11) occurs. Our approach based on the analysis of the dynamics of different time scales s gives analogous results. The behavior of the phase difference $\phi_{s1}(t) - \phi_{s2}(t)$ for this case is presented in Fig. 4*b*. One can see that phase locking occurs for the time scales $s = 5.25$, which are characterized by the largest energy value in the wavelet power spectra $\langle E(s)\rangle$ (Fig. 4*a*).

We note that the phase difference $\phi_{s1}(t) - \phi_{s2}(t)$ is also bounded at the time scales close to $s = 5.25$. We can say that the time scales $s = 5.25$ (and close to them) of two oscillators are synchronized with each other. At the same time, other time scales (e.g., $s = 4.5, 6.0$) remain uncorrelated. For such time scales, phase locking was not observed (see Fig. 4*b*).

It is clear that the mechanism of synchronization of coupled chaotic oscillators is the same in both cases considered in Sec. 3 and 4. The synchronization phenomenon is caused by the existence of time scales s in system dynamics correlated with each other. Therefore, there is no reason to divide the considered synchronization examples into different types.

It has been shown [21] that there is a certain relation between phase, lag, and complete synchronizations for chaotic oscillators with slightly mismatched parameters. With the increase of the coupling strength, the systems undergo the transition from unsynchronized chaotic oscillations to phase synchronization. With a further increase of the coupling, lag synchronization is observed. As of the coupling parameter increases further, the time lag decreases and both systems tend to have the complete synchronization regime.

We consider the dynamics of different time scales s of two nonidentical coupled Rössler systems (11) when the coupling parameter value increases. If there is no phase synchronization between the oscillators, their dynamics remain uncorrelated for all time scales s. Figure 5 illustrates the dynamics of two coupled Rössler systems when the coupling parameter ε is small enough ($\varepsilon = 0.025$). The power spectra $\langle E(s)\rangle$ of the wavelet transform for Rössler systems differ from each other (Fig. 5*a*), but the maximum values of the energy correspond approximately to the same time scale s in both systems. It is clear that the phase difference $\phi_{s1}(t) - \phi_{s2}(t)$ is not bounded for almost all time scales (Fig. 5*b*). One can see that the phase difference $\varphi_{s1}(t) - \varphi_{s2}(t)$ increases for the time scale $s = 3.0$, but decreases for $s = 4.5$. This means that there should be a time scale $3.0 < s^* < 4.5$ at which the phase difference remains bounded. This time scale s^* plays the role of a point separating the time scale areas with the phase difference increasing and decreasing, respec-

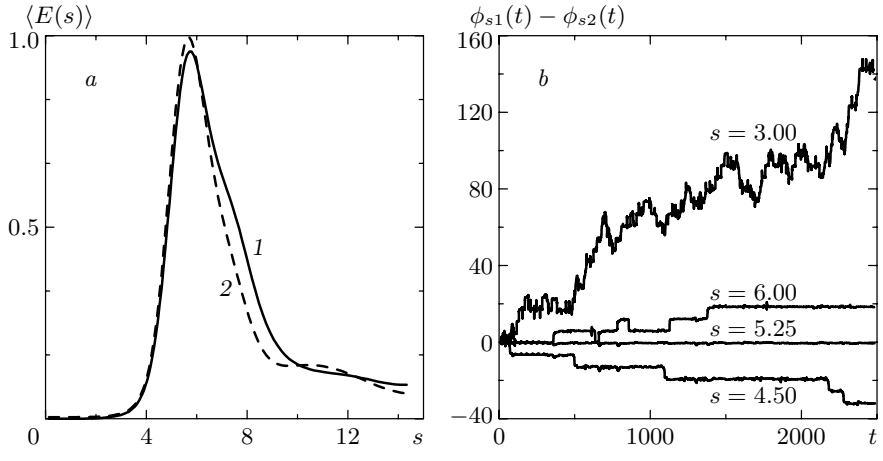

Fig. 4. (*a*) The normalized energy distribution in the wavelet spectrum $\langle E(s)\rangle$ for the first (line *1*) and the second (line *2*) Rössler systems (11); (*b*) the phase difference $\phi_{s1}(t) - \phi_{s2}(t)$ for two coupled Rössler systems. The value of the coupling parameter is selected as $\varepsilon = 0.05$. The time scales $s = 5.25$ are correlated with each other and synchronization is observed

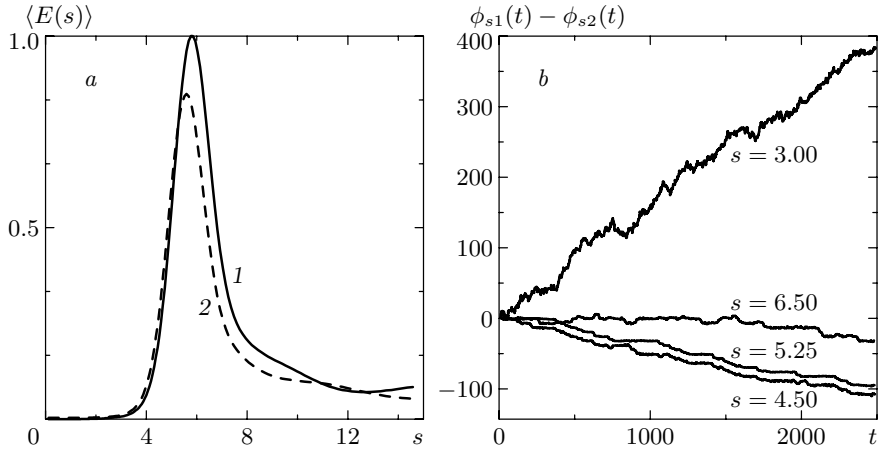

Fig. 5. (*a*) The normalized energy distribution in the wavelet spectrum $\langle E(s)\rangle$ for the first (line *1*) and the second (line *2*) Rössler systems; (*b*) the phase difference $\phi_{s1}(t) - \phi_{s2}(t)$ for two coupled Rössler systems. The value of coupling parameter is selected as $\varepsilon = 0.025$. There is no phase synchronization between the systems

tively. In this case, the measure of time scales at which the phase difference remains bounded is zero and we cannot speak about the synchronous behavior of coupled chaotic oscillators (see also Sec. 6).

As soon as any of the time scales of the first chaotic oscillator becomes correlated with another time scale of the second oscillator (e.g., when the coupling parameter increases), phase synchronization occurs (see Fig. 4). The time scales s characterized by the largest value of energy in the wavelet spectrum $\langle E(s)\rangle$ are more likely to become correlated first. The other time scales remain uncorrelated as before. The phase synchronization between chaotic oscillators leads to phase locking (3) at the correlated time scales s.

As the parameter of coupling between the chaotic oscillators increases, more and more time scales become correlated and one can say that the degree of synchronization grows. Therefore, with the further increase of the coupling parameter value (e.g., $\varepsilon = 0.07$) in coupled Rössler systems (11), the time scales that were uncorrelated before become synchronized (Fig. 6*b*). It is evident that the time scales $s = 4.5$ are synchronized in comparison with the previous case ($\varepsilon = 0.05$, Fig. 4*b*) when these time scales were uncorrelated. The number of time scales s demonstrating phase locking increases, but there are nonsynchronized time scales as before (e.g., the time scales $s = 3$ and $s = 6$ remain nonsynchronized).

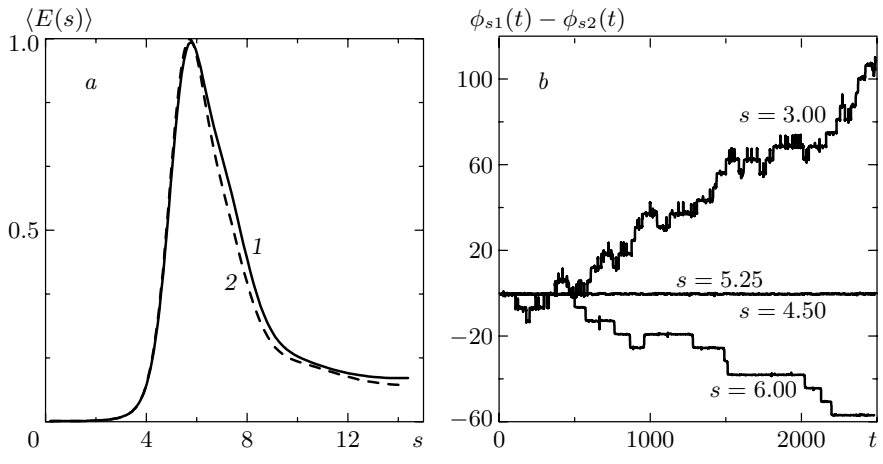

Fig. 6. (a) The normalized energy distribution in the wavelet spectrum $\langle E(s)\rangle$ for the first (line *1*) and the second (line *2*) Rössler systems; (b) the phase difference $\phi_{s1}(t) - \phi_{s2}(t)$ for two coupled Rössler systems. The value of coupling parameter is selected as $\varepsilon = 0.07$

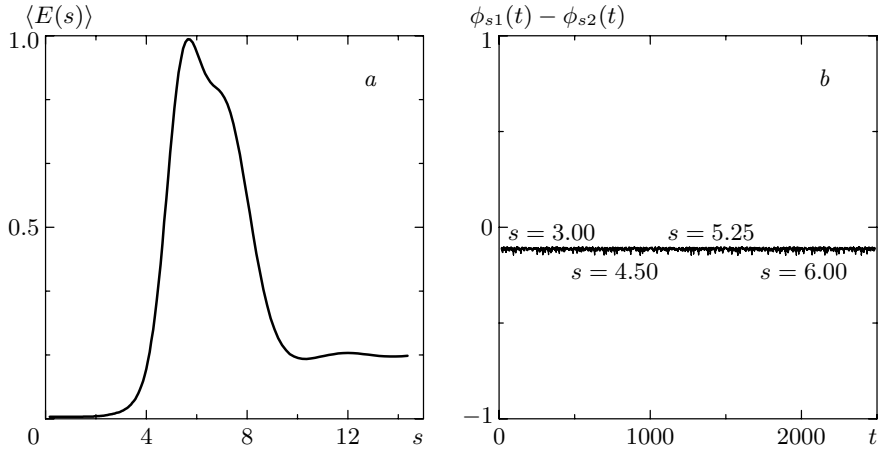

Fig. 7. (a) The normalized energy distribution in the wavelet spectrum $\langle E(s)\rangle$ for the Rössler system; (b) the phase difference $\phi_{s1}(t) - \phi_{s2}(t)$ for two coupled Rössler systems. The value of the coupling parameter is selected as $\varepsilon = 0.25$. Lag synchronization is observed, all time scales are synchronized

The occurrence of lag synchronization [21] between oscillators means that all time scales are correlated. Indeed, the lag-synchronization condition $x_1(t-\tau) \approx x_2(t)$ implies that $W_1(s, t-\tau) \approx W_2(t, s)$ and therefore $\phi_{s1}(t-\tau) \approx \phi_{s2}(t)$. In this case, phase locking condition (3) is obviously satisfied for all time scales s. For instance, when the coupling parameter of chaotic oscillators (11) becomes large enough ($s = 0.25$), lag synchronization of two coupled oscillators occurs. In this case, the power spectra of the wavelet transform coincide with each other (see Fig. 7a) and phase locking takes place for all time scales s (Fig. 7b). We note that the phase difference $\phi_{s1}(t) - \phi_{s2}(t)$ is not equal to zero in the case of lag synchronization. It is clear that this difference depends on the time lag τ.

A further increase of the coupling parameter leads to a decrease of the time lag τ [21]. Both systems tend to have the complete synchronization regime $x_1(t) \approx x_2(t)$, and hence the phase difference $\phi_{s1}(t) - \phi_{s2}(t)$ tends to be zero for all time scales.

The dependence of the synchronized time scale range $[s_m; s_b]$ on the coupling parameter is shown in Fig. 8. The range $[s_m; s_b]$ of synchronized time scales appears at $\varepsilon \approx 0.039$. The appearance of the synchronized time scale range corresponds to the phase synchronization regime. As the coupling parameter value increases, the range of synchronized time scales ex-

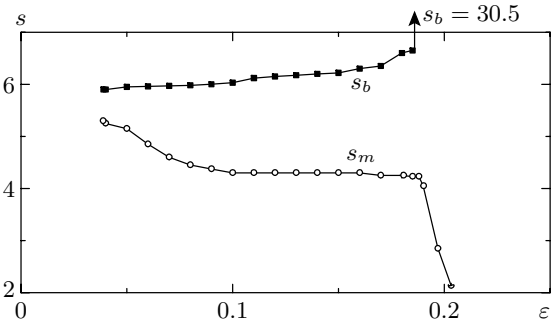

Fig. 8. The dependence of the synchronized time scale range $[s_m; s_b]$ on the coupling strength ε for two coupled Rössler systems (11) with funnel attractors

pands until all time scales become synchronized. Synchronization of all time scales means the presence of the lag synchronization regime.

We can therefore say that the time-scale synchronization is the most general synchronization type unifying (at least) the phase, lag, and complete synchronization regimes.

5. GENERALIZED SYNCHRONIZATION REGIME

We consider another type of synchronized behavior, the so-called generalized synchronization. It has been shown above that phase, lag, and complete synchronizations are naturally related to each other and the synchronization type depends on the number of synchronized time scales. The details of the relations between phase and generalized synchronizations are not clear at all. There are several works [1, 22] dealing with the problem of how phase and generalized synchronizations are correlated with each other. For instance, it has been reported in [22] that two unidirectional coupled Rössler systems can demonstrate the generalized synchronization, while the phase synchronization has not been observed. This case can easily be explained by means of the time scale analysis. The equations of the Rössler system are

$$\begin{aligned} \dot{x}_1 &= -\omega_1 y_1 - z_1, \\ \dot{y}_1 &= \omega_1 x_1 + a y_1, \\ \dot{z}_1 &= p + z_1(x_1 - c) \\ \dot{x}_2 &= -\omega_2 y_2 - z_2 + \varepsilon(x_1 - x_2), \\ \dot{y}_2 &= \omega_2 x_2 + a y_2, \\ \dot{z}_2 &= p + z_2(x_2 - c), \end{aligned} \tag{12}$$

where $\mathbf{x}_1 = (x_1, y_1, z_1)^T$ and $\mathbf{x}_2 = (x_2, y_2, z_2)^T$ are the respective state vectors of the first (drive) and the second (response) Rössler systems. The control parameter values are chosen as $\omega_1 = 0.8$, $\omega_2 = 1.0$, $a = 0.15$, $p = 0.2$, $c = 10$, and $\varepsilon = 0.2$. Generalized synchronization occurs in this case (see [22] for details). The time scale analysis explains why it is impossible to detect phase synchronization in system (12) despite generalized synchronization being observed.

We consider Fourier spectra of coupled chaotic oscillators (Fig. 9). There are two main spectral components with the frequencies $f_1 = 0.125$ and $f_2 = 0.154$ in these spectra. The analysis of the behavior of time scales showns that both the time scales $s_1 = 1/f_1 = 8.0$ of the coupled oscillators corresponding to the frequency f_1 and time scales close to s_1 are synchronized, while the time scales $s_2 = 1/f_2 \approx 6.5$ and those close to this value do not demonstrate synchronous behavior (Fig. 10*b*).

The source of such behavior of time scales becomes clear from the wavelet power spectra $\langle E(s) \rangle$ of both systems (see Fig. 10*a*). The time scale s_1 of the drive Rössler system is characterized by a large value of energy, while the part of energy associated with this scale of the response system is quite small. Therefore, the drive system dictates its own dynamics at the time scale s_1 to the response system. The opposite situation occurs for the time scales s_2 (Fig. 10*a*). The drive system cannot dictate its dynamics to the response system because the part of energy associated with this time scale is small in the first Rössler system and large enough in the second one. Therefore, time scales s_2 are not synchronized.

Thus, the generalized synchronization of the unidirectional coupled Rössler systems appears as the time scale synchronized dynamics, similarly to other synchronization types. It is also clear why the phase synchronization was not observed in this case. Figure 9 shows that the instantaneous phases $\phi_{1,2}(t)$ of chaotic signals $\mathbf{x}_{1,2}(t)$ introduced by means of traditional approaches are determined by both frequencies, f_1 and f_2, but only the spectral components with the frequency f_1 are synchronized. Therefore, observation of the instantaneous phases $\phi_{1,2}(t)$ does not allow detecting phase synchronization in this case although the synchronization of time scales takes place.

Thus, one can see that there is a close relation between different types of the chaotic oscillator synchronization. According to the results mentioned above, we can say that phase, lag, complete, and generalized synchronizations are particular cases of time-scale synchronization. Therefore, it is possible to consider differ-

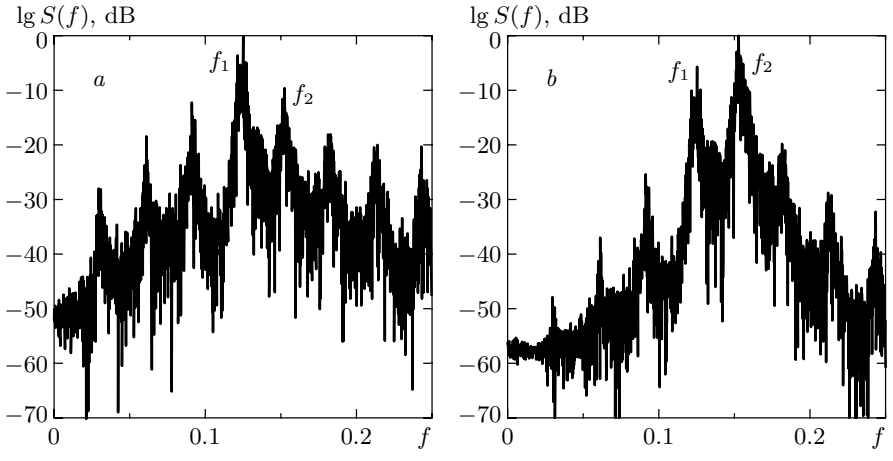

Fig. 9. Fourier spectra for (a) the first (drive) and (b) the second (response) Rösler systems (12). The coupling parameter is $\varepsilon = 0.2$. Generalized synchronization occurs

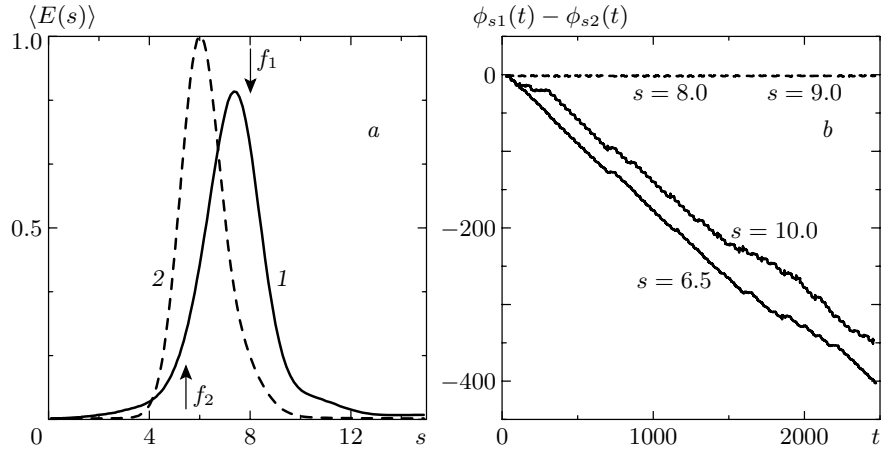

Fig. 10. (a) The normalized energy distribution in the wavelet spectrum $\langle E(s)\rangle$ for the first (line *1*) and the second (line *2*) Rössler systems. The time scales indicated with arrows correspond to the frequencies $f_1 = 0.125$ and $f_2 = 0.154$; (b) the phase difference $\phi_{s1}(t) - \phi_{s2}(t)$ for two coupled Rössler systems. The generalized synchronization is observed

ent types of synchronized behavior from the universal standpoint. Unfortunately, it is not clear how one can distinguish the phase synchronization[1)] and the generalized synchronization using only the results obtained from the analysis of the time scale dynamics.

6. MEASURE OF SYNCHRONIZATION

From the examples given above, we can see that any type of synchronous behavior of coupled chaotic oscillators leads to the occurrence of synchronized time scales. Therefore, the measure of synchronization can be introduced. This measure ρ can be defined as the part of the wavelet spectrum energy associated with the synchronized time scales,

$$\rho_{1,2} = \frac{1}{E_{1,2}} \int\limits_{s_m}^{s_b} \langle E_{1,2}(s)\rangle \, ds, \tag{13}$$

where $[s_m; s_b]$ is the range of time scales for which condition (1) is satisfied and

$$E_{1,2} = \int\limits_{0}^{+\infty} \langle E_{1,2}(s)\rangle \, ds \tag{14}$$

is the total energy of the wavelet spectrum. This measure ρ is zero for the nonsynchronized oscillations and

[1)] We here mean that phase synchronization between chaotic oscillators occurs if the instantaneous phase $\phi(t)$ of the chaotic signal may be correctly introduced by means of traditional approaches and phase locking condition (1) is satisfied.

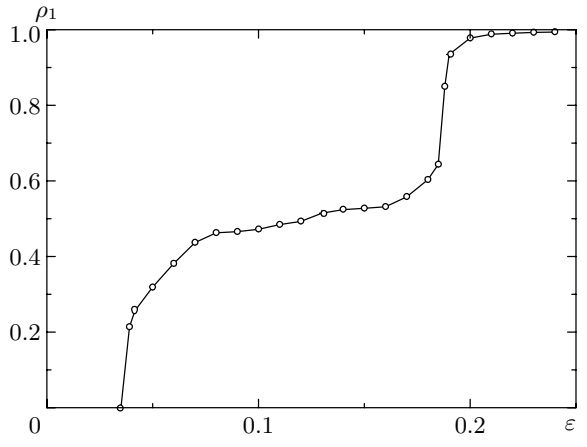

Fig. 11. The dependence of the synchronization measure ρ_1 for the first Rössler system (11) on the coupling strength ε. The measure ρ_2 for the second Rössler oscillator behaves in a similar manner (not shown in the figure)

unity for the complete and lag synchronization regimes. If the phase synchronization regime is observed, ρ takes a value between zero and unity depending on the part of energy associated with the synchronized time scales. Hence, the synchronization measure ρ allows not only distinguishing the synchronized and nonsynchronized oscillations, but also characterizing the degree of time-scale synchronization quantitatively.

Figure 11 presents the dependence of the TSS synchronization measure ρ_1 for the first Rössler oscillator of system (11) considered in Sec. 4 on the coupling parameter ε. It is clear that the part of the energy associated with the synchronized time scales grow monotonically with the growth of the coupling strength. Similar results have been obtained for the generalized synchronization of two coupled Rössler systems considered in Sec. 5.

We have already mentioned that when the coupled oscillators do not demonstrate synchronous behavior, there are time scales s^* at which the phase difference $\varphi_{s1}(t) - \varphi_{s2}(t)$ is bounded. Such time scales play the role of points separating the time scale areas where the phase difference increases and decreases, respectively (see also Sec. 4). Nevertheless, the presence of such time scales does not mean the occurrence of chaotic synchronization because the part of energy associated with them is equal to zero. Therefore, the synchronization measure ρ of such oscillations is zero, and the dynamical regime realized in the system in this case should be classified as nonsynchronous.

7. CONCLUSIONS

Summarizing this work, we note several principal aspects. First, we have proposed to consider the time scale dynamics of coupled chaotic oscillators. It allows us to consider the different types of behavior of coupled oscillators (such as the complete synchronization, the lag synchronization, the phase synchronization, the generalized synchronization, and the nonsynchronized oscillations) from the universal standpoint. In this case, time-scale synchronization is the most common type of synchronous coupled chaotic oscillator behavior. Therefore, the other types of synchronous oscillations (phase, lag, complete, and generalized) may be considered the particular cases of time-scale synchronization. The quantitative characteristic ρ of the synchronization measure has also been introduced. It is important to note that our method (with insignificant modifications) can also be applied to dynamical systems synchronized by the external (e.g., harmonic) signal.

Second, the traditional approach for the phase synchronization detecting based on the introduction of the instantaneous phase $\phi(t)$ of the chaotic signal is suitable and correct for such time series characterized by the Fourier spectrum with a single main frequency f_0. In this case, the phase ϕ_{s0} associated with the time scale s_0 corresponding to the main frequency f_0 of the Fourier spectrum coincides approximately with the instantaneous phase $\phi(t)$ of the chaotic signal introduced by means of the traditional approaches (see also [36]). Indeed, because the other frequencies (the other time scales) do not play a significant role in the Fourier spectrum, the phase $\phi(t)$ of the chaotic signal is close to the phase $\phi_{s0}(t)$ of the main spectral frequency f_0 (and the main time scale s_0, respectively). It is obvious that in this case, the mean frequencies $\bar{f} = \langle\dot{\phi}(t)\rangle/2\pi$ and $\bar{f}_{s0} = \langle\dot{\phi}_{s0}(t)\rangle/2\pi$ should coincide with each other and with the main frequency f_0 of the Fourier spectrum (see also [31]),

$$\bar{f} = \bar{f}_{s0} = f_0. \tag{15}$$

If the chaotic time series is characterized by the Fourier spectrum without a single basic frequency (like the spectrum shown in Fig. 3*b*), the traditional approaches fail. One has to consider the dynamics of the system at all time scales, but this cannot be done by means of the instantaneous phase $\phi(t)$. On the contrary, our approach based on the analysis of time scale dynamics can be used for both types of chaotic signals.

Finally, our approach can be easily applied to the experimental data because it does not require any *a priori* information on the considered dynamical systems. Moreover, in several cases, the influence of the noise can be reduced by means of the wavelet transform (see [39, 48, 49] for details). We believe that our approach will be useful and effective for the analysis of physical, biological, physiological, and other data, such as described in [10, 36, 35].

We thank D. I. Trubetskov, V. S. Anishchenko, and T. E. Vadivasova for valuable discussions. We also thank S. V. Eremina for support.

This work has been supported by the CRDF (grant REC-006) and the RFBR (grant 02-02-16351). One of the authors (A. E. H.) also thanks the «Dynastiya» Foundation.

REFERENCES

1. U. Parlitz, L. Junge, and W. Lauterborn, Phys. Rev. E **54**, 2115 (1996).
2. D. Y. Tang, R. Dykstra, M. W. Hamilton, and N. R. Heckenberg, Phys. Rev. E **57**, 3649 (1998).
3. E. Allaria, F. T. Arecchi, A. D. Garbo, and R. Meucci, Phys. Rev. Lett. **86**, 791 (2001).
4. C. M. Ticos, E. Rosa, W. B. Pardo et al., Phys. Rev. Lett. **85**, 2929 (2000).
5. E. Rosa, W. B. Pardo, C. M. Ticos et al., Int. J. Bifurcations and Chaos **10**, 2551 (2000).
6. D. I. Trubetskov and A. E. Hramov, J. Comm. Technol. Electron. **48**, 105 (2003).
7. P. A. Tass, M. G. Rosenblum, J. Weule et al., Phys. Rev. Lett. **81**, 3291 (1998).
8. V. S. Anishchenko, A. G. Balanov, N. B. Janson et al., Int. J. Bifurcations and Chaos **10**, 2339 (2000).
9. M. D. Prokhorov, V. I. Ponomarenko, V. I. Gridnev et al., Phys. Rev. E **68**, 041913 (2003).
10. R. C. Elson, A. I. Selverston, R. Huerta et al., Phys. Rev. Lett. **81**, 5692 (1998).
11. N. F. Rulkov, Phys. Rev. E **65**, 041922 (2002).
12. P. A. Tass, Phys. Rev. Lett. **90**, 088101 (2003).
13. A. Pikovsky, M. Rosenblum, and J. Kurths, *Synchronization: a Universal Concept in Nonlinear Sciences*, Cambridge University Press (2001).
14. A. Pikovsky, M. Rosenblum, and J. Kurths, Int. J. Bifurcations and Chaos **10**, 2291 (2000).
15. V. S. Anishchenko and T. E. Vadivasova, J. Comm. Technol. Electron. **47**, 117 (2002).
16. V. S. Anshchenko, V. Astakhov, A. Neiman, T. Vadivasova, and L. Schimansky-Geier, *Nonlinear Dynamics of Chaotic and Stochastic Systems. Tutorial and Modern Developments*, Springer-Verlag, Heidelberg (2001).
17. L. M. Pecora and T. L. Carroll, Phys. Rev. Lett. **64**, 821 (1990).
18. L. M. Pecora and T. L. Carroll, Phys. Rev. A **44**, 2374 (1991).
19. K. Murali and M. Lakshmanan, Phys. Rev. E **49**, 4882 (1994).
20. K. Murali and M. Lakshmanan, Phys. Rev. E **48**, R1624 (1994).
21. M. G. Rosenblum, A. S. Pikovsky, and J. Kurths, Phys. Rev. Lett. **78**, 4193 (1997).
22. Z. Zheng and G. Hu, Phys. Rev. E **62**, 7882 (2000).
23. S. Taherion and Y. C. Lai, Phys. Rev. E **59**, R6247 (1999).
24. N. F. Rulkov, M. M. Sushchik, L. S. Tsimring, and H. D. I. Abarbanel, Phys. Rev. E **51**, 980 (1995).
25. L. Kocarev and U. Parlitz, Phys. Rev. Lett. **76**, 1816 (1996).
26. K. Pyragas, Phys. Rev. E **54**, R4508 (1996).
27. M. G. Rosenblum, A. S. Pikovsky, and J. Kurths, Phys. Rev. Lett. **76**, 1804 (1996).
28. G. V. Osipov, A. S. Pikovsky, M. G. Rosenblum, and J. Kurth, Phys. Rev. E **55**, 2353 (1997).
29. H. D. I. Abarbanel, N. F. Rulkov, and M. Sushchik, Phys. Rev. E **53**, 4528 (1996).
30. L. M. Pecora, T. L. Carroll, and J. F. Heagy, Phys. Rev. E **52**, 3420 (1995).
31. V. S. Anishchenko and T. E. Vadivasova, J. Comm. Technol. Electron. **49**, 69 (2004).
32. A. Pikovsky, M. Rosenblum, G. Osipov, and J. Kurths, Physica D **104**, 219 (1997).
33. M. G. Rosenblum, A. S. pikovsky, and J. Kurths, Phys. Rev. Lett. **89**, 264102 (2002).
34. G. V. Osipov, B. Hu, C. Zhou et al., Phys. Rev. Lett. **91**, 024101 (2003).

35. J. P. Lachaux, E. Rodriguez, M. V. Quyen et al., Int. J. Bifurcations and Chaos **10**, 2429 (2000).

36. R. Q. Quiroga, A. Kraskov, T. Kreuz, and P. Grassberger, Phys. Rev. E **65**, 041903 (2002).

37. A. S. Pikovsky, M. G. Rosenblum, and J. Kurths, Europhys. Lett. **34**, 165 (1996).

38. A. A. Koronovskii and A. E. Hramov, Pis'ma v Zh. Eksp. Teor. Fiz. **79**, 391 (2004).

39. A. A. Koronovskii and A. E. Hramov, *Continuous Wavelet Analysis and its Applications* (*in Russian*) Fizmatlit, Moscow (2003).

40. I. Daubechies, *Ten Lectures on Wavelets*, SIAM (1992).

41. G. Kaiser, *A Friendly Guide to Wavelets*, Springer-Verlag, New York (1994).

42. B. Torresani, *Continuous Wavelet Transform*, Savoire, Paris (1995).

43. A. Lutz, D. Rudrauf, D. Cosmelli et al., Neurophysiol. Clin. **32**, 157 (2002).

44. M. L. V. Quyen, J. Martinerie, C. Adam, and F. J. Varela, J. Neurosci. Meth. **111**, 83 (2001).

45. D. J. De Shazer., R. Breban, E. Ott, and R. Roy, Phys. Rev. Lett. **87**, 044101 (2001).

46. O. V. Sosnovtseva, A. N. Pavlov, E. Mosekilde, and N.-H. Holstein-Rathlou, Phys. Rev. E **66**, 061909 (2002).

47. A. Grossman and J. Morlet, SIAM J. Math. Anal. **15**, 273 (1984).

48. C. Torrence and G. P. Compo, Bull. Amer. Meteorol. Soc. **79**, 61 (1998).

49. V. A. Gusev, A. A. Koronovskiy, and A. E. Hramov, Pis'ma v Zh. Eksp. Teor. Fiz. **29** (18), 61 (2003).